J. Electrochem. Sci. Eng. **15(5)** (2025) 2546; http://dx.doi.org/10.5599/jese.2546

Open Access : : ISSN 1847-9286
https://pub.iapchem.org/ojs/index.php/JESE

Original scientific paper

Original hydrazine carbothioamide Schiff base derivative as a suitable mitigator for corrosion of carbon steel and hydrogen production in acidic aqueous media

Mahmoud G. A. Saleh[1,✉], Majda Alfaker[2,✉], Rasha N. Felaly[3], Salih S. Al-Juaid[4], Fatima H. Alabdali[5], Kamal A. Soliman[6], Metwally Abdallah[6] and Salah Abd El Wanees[7,✉]

[1]*Chemistry Department, College of Science, Northern Border University, Arar, Saudi Arabia*
[2]*Chemistry Department, Faculty of Science, Prince Nourah bint Abdulrahman University, Riyadh, Saudi Arabia*
[3]*Chemistry Department, Faculty of Science, Umm Al-Qura University, Makkah, Saudi Arabia*
[4]*Chemistry Department, Faculty of Science, King Abdulaziz University, Jeddah, Saudi Arabia*
[5]*Al Qunfudhah University College, Umm Al-Qura University, Saudi Arabia*
[6]*Chemistry Department, Faculty of Science, Benha University, Benha, Egypt*
[7]*Chemistry Department, Faculty of Science, Zagazig University, Zagazig, Egypt*

Corresponding authors: ✉mahmoud.saleh2@nbu.edu.sa, ✉msalonazi@pnu.edu, ✉s_wanees@yahoo.com

Received: October 26, 2024; Accepted: June 19, 2025; Published: July 9, 2025

Abstract

The inhibitive effect of E-2-(1-methylpyrrolidin-2-ylidene) hydrazine carbo-thioamide Schiff base (MPHCA) towards the corrosion of carbon steel in hydrochloric acid media was examined using various chemical and electrochemical techniques. The rate of metal destruction in the HCl solution is reduced in the presence of the MPHCA. The inhibition efficiency is increased with more additions of MPHCA to reach 97.68 % at 5.0 mM concentration, at 25 °C. The inhibition process is controlled by the adsorption of inhibitive molecules on the carbon steel surface, obeying the Langmuir model. The computed ΔG^{o}_{ads} *values with the negative sign confirm the spontaneous nature of the adsorption process. Such values varied between -34.45 and -36.77 kJ mol*$^{-1}$*, supporting the mixed chemo and physisorption mechanisms. The lowering in* K_{ads} *values with the increase in temperature could confirm the escape of a few adsorbed MPHCA molecules from the metallic surface into the examined solution. The theoretical studies by the DFT method and conductor-like polarizable continuum determined the inhibitor's optimized geometries, providing insights into their molecular structure and potential properties. Monte Carlo and molecular dynamics simulations assessed the inhibitors' adsorption energy and comprehensive adsorption characteristics. MPHCA showed the highest adsorption energy, suggesting superior corrosion inhibition characteristics.*

Keywords
Iron-carbon alloy; corrosion inhibition; imine compound; mass loss; potentiodynamic polarization; hydrogen evolution; quantum computation

Introduction

Various industrial applications of carbon steel in oil and gas fields because to its reputable mechanical characteristics, besides the relative decrease in the cost of production [1]. Hydrochloric acid is typically used to remove undesired materials, rust, and sediment from various steel equipment. Dilute hydrochloric acid is used considerably in metal pickling. The lack of mineral acid use leads to the deterioration of the examined metallic surfaces, resulting in the waste of metallic resources [2]. Eco-friendly inhibitors inhibit the destructive influence of corrosive acids on metallic surfaces [3]. The choice of organic compounds to be used as inhibitors to retard the destruction of metals can largely depend on its frugal utilization and the presence of heteroatoms such as N, S, or O in their molecules, which should be environmentally harmless [4-12]. Schiff bases have been widely investigated as corrosion inhibitors for various metallic surfaces in acidic solutions, owing to the ease of synthesis from relatively inexpensive raw materials [12]. Nowadays, researchers have paid close attention to developing non-toxic, environmentally friendly inhibitors to protect metals from corrosion in acidic solutions. A Schiff base containing a C=N azomethine functional group, resulting from the condensation between an amine and a ketone or aldehyde, has been shown to provide better inhibition performance compared to corresponding amines [13]. The inhibiting influence of such inhibitors was found to depend on the adsorption of their molecules *via* active centres on the examined metal. Our early investigation proved that N^1, $N^{1'}$-(ethane-1,2-diyl)bis(N^2-(4-dimethylamino) benzylidene)ethane--1,2-diamine) behaves as an effective inhibitor towards the corrosion of C-steel in acidic medium with protection efficiency reaching 95.2 % at 5mM and 298 K [14].

Schiff bases are a vast group of compounds characterized by an azomethine group containing the -C=N- bond that could be synthesized by a dehydration process between an amine and a keto-aromatic compound [15]. Ferkous *et al*. [16] utilized 2-(2-methoxybenzylidene)hydrazine-1-carbothioamide as an excellent mitigator against the destruction of mild steel in a dilute hydrochloric acid medium. They indicated that such a compound exhibits good corrosion protection that reaches 98 % at optimum concentration, 2.0 mM, at 25 °C. The inhibition performance was dependent on the hetero atoms, which act as active adsorption centres owing to the presence of lone pairs of free electrons that can bind with the metallic surface. The gravimetric and electrochemical measurements indicated that the (*E*)-5-(4-(dimethylamino)phenyl)-3-(4-(dimethylamino)styryl)-2,3-dihydro--1*H*-pyrazole-1-carbothioamide exhibits good inhibition, ascribed to chemisorption and physisorption [17]. The potentiodynamic polarization of carbon steel in HCl solutions confirmed that 2-(2,4,5-trimethoxy-benzylidene)hydrazine carbothioamide behaves as a mixed-type inhibitor [18]. The Nyquist plots indicated a rise in the charge transfer resistance with a lower double-layer capacitance by an increase in the inhibitor concentration in the corrosive solution [18]. The 2,2'-(1,4-phenylene bis (methanilylidene)) bis(N-(3-methoxyphenyl) hydrazine-carbothioamide) was examined as an effective mitigator to decrease the destruction of steel in dilute hydrochloric acid media. The efficiency of the protection exceeds 95% in the presence of 0.5 mM of this inhibitor. The inhibition of the metal destruction process is favored by increasing the added amount of the inhibitor and is reduced with the increase in the solution temperature. The inhibition is controlled by the adsorption process that obeys the Langmuir isotherm. The data on the free energy of adsorption illustrated the existence of physical and chemical adsorption [18].

New Schiff base inhibitors were prepared to mitigate corrosion of the carbon steel in dilute hydrochloric acid solutions [14,19]. The protection efficiency reached 97% at a concentration of 0.005 M, at 25 °C, indicating the existence of a mixed adsorption mechanism. In this study, eco-friendly non-toxic Schiff base inhibitor, namely, (*E*)-2-(1-methylpyrrolidin-2-ylidene) hydrazine carbothioamide, MPHCA, was synthesized to investigate the protective influence against the corrosion of the carbon steel in dilute hydrochloric acid solutions. The MPHCA compound is considered a neutral compound that is readily soluble in HCl solutions without influencing the conductivity and pH of the solution. Different experimental studies were performed to deduce the inhibition efficiencies of the MPHCA compound in the examined acidic solutions. The inhibition mechanism was examined through an adsorption process at different temperatures. Various thermodynamic functions accompanied by the corrosion and inhibition processes are computed and discussed.

Density functional theory, DFT, and molecular dynamics, MD, simulations are powerful computational methods utilized to predict the model of the adsorption attitude of the utilized inhibitor on the examined metal [20]. Such techniques enable the study of how structural parameters of the MPHCA molecule affect the efficiency as a corrosion inhibitor by examining the electronic properties and electron density apportionment derived from DFT calculations. In addition, MD simulations offer insights into the adsorption characteristics linked to corrosion inhibition efficiency through molecular modelling. By utilizing these simulations, researchers can analyse the interactions between inhibitors and metal surfaces, which can help to optimize the design of more effective organic compounds as corrosion inhibitors.

Experimental

Electrodes and chemicals

The samples required for gravimetric and gasometric analysis and the working electrode (WE) needed for electrochemical investigations, were cut from C-steel with elemental analysis similar to that reported earlier [14]. The WE was prepared in the form of a small roller bar of C-steel embedded in epoxy resin with a polytetrafluoroethylene coating, having a free cross-sectional area of 0.38 cm². The samples were mechanically polished using different grades of polishing papers, starting with a coarser grade and progressing to finer grades [14]. The chemicals required for the synthesis process are 1-methylpyrrolidin-2-one and benzo[d]thiazol-2-amine ethanolic, which were purchased from Meric Chemicals with a purity exceeding 99 %.

Synthesis of MPHCA compound

The objective of the preparation of *N*-(1-methylpyrrolidin-2-ylidene) benzo[d]- thiazol-2-amine Schiff base, MPHCA, was to examine the protection of steel from corrosion processes in hydrochloric acid media. The synthesis process depicted in Scheme 1, was performed by mixing 0.1 moles of 1-methylpyrrolidin-2-one ethanolic solution with 0.1 moles of benzo[d]thiazol-2-amine ethanolic solution in a 250 ml three-necked flask. The content of the flask was heated by stirring with a reflux for 5 hours. The product of the solution was evaporated to get rid of the solvent, followed by a washing process various times, and recrystallized from ethanolic solvent. The molecular weight of the produced compound was determined to be 219.28 g mol^{-1}.

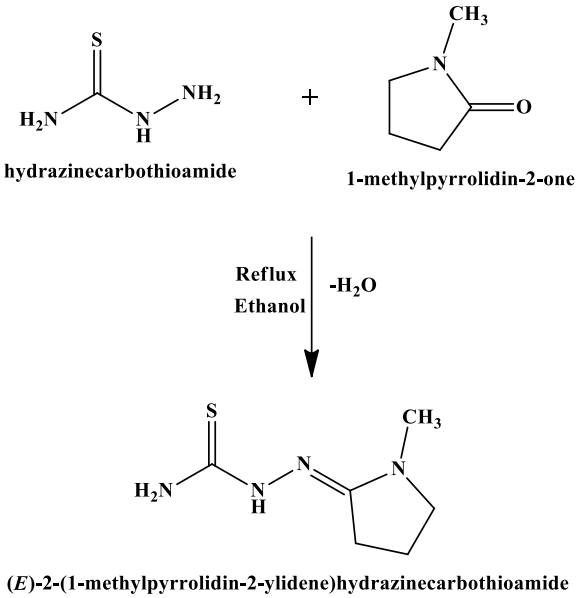

Scheme 1. *Synthesis of (E)-2-(1-methylpyrrolidin-2-ylidene) hydrazinecarbothioamide, MPHCA, inhibitor*

Mass loss investigation

The samples of carbon steel required for mass loss measurements were cut and prepared as reported in the previous work [14]. The dry-cleaned metallic sample with dimensions 7.6×2.2×0.3 cm was weighed using a highly precise laboratory balance (with readability 0.1 mg), giving a weight W_1. Such a prepared metallic sample was immersed in 250 ml of the aggressive or inhibitive test solution for 8 h. The investigated sample of C-steel is locked onto the examined solution, dried, and reweighed, yielding a weight of W_2. Each experiment was repeated three times, and the average value was determined.

The rate of metallic corrosion (r_g) was determined by Equation (1) [21]:

$$r_g = \frac{\Delta W}{At} \quad (1)$$

where $\Delta W = W_1 - W_2$, t / h is the immersion period, and A is the contact area of the metallic surface. The obtained values of r_g were used to deduce the surface coverage (θ) and the protection efficiency (η_w) of the MPHCA inhibitor by Equations (2) and (3) [9]:

$$\theta = \left(1 - \frac{r_g}{r^o_g}\right) \quad (2)$$

$$\eta_w = \left(1 - \frac{r_g}{r^o_g}\right)100 \quad (3)$$

where r^o_g and r_g are the corrosion reaction rates of carbon steel in HCl solutions without and with added MPHCA compound, respectively.

Gasometry study

The vessel and experimental procedure for hydrogen evolution measurements have been described earlier [22,23]. The C-steel coupons were cut to the exact dimensions of 7.6×2.2×0.3 cm. All samples were polished with fine polishing papers and cleaned by washing under running tap water, then ultrasonically cleaned in distilled water, and finally dried before immersion in the examined solution. After an induction period, the produced hydrogen begins to increase with immersion time, being collected over water. The V-time curves of C-steel in 1.0 M HCl, free of, and mixed with various amounts of MPHCA inhibitor, were constructed. The data of the volume (V) of

the produced H_2 at various immersion times (τ) were used to deduce the rate of the metal destruction, r_H. The values r_H were used to deduce the values of θ and η_H *via* Equations (4) and (5) [23]:

$$\theta = \left(1 - \frac{r_H}{r^o_H}\right) \quad (4)$$

$$\eta_H = \left(1 - \frac{r_H}{r^o_H}\right)100 \quad (5)$$

where r^o_H and r_H are corrosion reaction rates expressed by the rates of hydrogen production in 1.0 M hydrochloric acid-free and mixed with various additions of the MPHCA inhibitor, respectively.

Electrochemical study

The electrochemical potentiodynamic polarization (PD) and electrochemical impedance spectra measurements (EIS) [20] were used to confirm the protection effect of the MPHCA towards corrosion of the carbon steel in HCl solution. The used electrolytic cell contains three electrodes: carbon steel as a working electrode, WE, a Pt plate as an auxiliary electrode, and a saturated calomel, SCE, as a reference electrode. The WE was prepared by mechanical polishing using various grades of abrasive paper, similar to those indicated previously [14]. The polarization data were recorded when the potential, *E*, of the WE was swept with a scan rate of 0.2 mV s^{-1} between -850 and -350 mV *vs.* SCE, starting from the steady state potential, at 25 °C using a voltaLab potentiostat PGZ 301 model.

The corrosion current density gained in the corrosive solution (j^o_{corr}) and in the inhibitive solution (j_{corr}) were computed by extrapolation of anodic and cathodic Tafel slopes. The values of θ and inhibition efficiency (η_p) were deduced from Equations (6) and (7) [24]:

$$\theta = \left(1 - \frac{j_{corr}}{j^o_{corr}}\right) \quad (6)$$

$$\eta_p = \left(1 - \frac{j_{corr}}{j^o_{corr}}\right)100 \quad (7)$$

The EIS study was done on carbon steel electrodes in the corrosive and inhibitive solutions at E_{corr} and frequencies (f) varied between 100 kHz and 50 mHz with an amplitude of 0.01 V. The data of the EIS plots were fitted utilizing the ZSimpWin approach [25].

The charge transfer resistances, R^o_{ct} for the corrosive acid solution, and R_{ct} for the inhibitive acid solution, were used to compute the values of θ, and the inhibition efficiency (η_I) utilizing Equations (8) and (9):

$$\theta = \left(1 - \frac{R^o_{ct}}{R_{ct}}\right) \quad (8)$$

$$\eta_{I=} \left(1 - \frac{R^o_{ct}}{R_{ct}}\right)100 \quad (9)$$

Utilizing $\omega_{max} = 2\pi f_{max}$, the double-layer capacitance, C_{dl}, can be deduced using Equation (10) [26]

$$C_{dl} = Y^o \omega_{max}^{n-1} \quad (10)$$

where Y^o is a proportional factor and n is the phase shift.

Surface investigation

The surface morphology of corroded and uncorroded carbon steel samples in the examined solutions can be investigated utilizing a scanning electron microscope, SEM. A clean steel sample

was examined under SEM before immersion in the test solution. The other samples were investigated after immersion for 4 hours in 1.0 M HCl, free of and mixed with 0.005 M of the MPHCA compound, at 25 °C.

Quantum computations

The density functional theory (DFT) computations were conducted utilizing Gaussian 09 software [27] to evaluate the behaviour of the MPHCA compound as a corrosion inhibitor. These computations included geometry optimizations of the inhibitors using the B3LYP method, which combines Becke's three-parameter functional (B3) with the gradient-corrected correlation LYP functional. The 6-31G(d,p) basis set was applied for all atoms in the calculations.

The theoretical evaluation of inhibitor compounds enables a detailed analysis of intermolecular forces and global chemical reactivity indicators, such as the highest occupied molecular orbital (E_{HOMO}), lowest unoccupied molecular orbital (E_{LUMO}), and energy gap (ΔE), particularly through CPCM solvation.

Global hardness (η), softness (σ), and the number of electrons transferred (N) can be computed by Equations (11) to (13):

$$\eta = \left(\frac{E_{LUMO} - E_{HOMO}}{2} \right) \quad (11)$$

$$\sigma = \frac{1}{\eta} \quad (12)$$

$$\Delta N_{110} = \left(\frac{\varphi - \chi_{inh}}{2(\eta_{Fe} + \eta_{inh})} \right) \quad (13)$$

where φ, χ_{inh}, η_{Fe} and η_{inh} are the work functions of Fe (110) (4.82 eV) [27], the electronegativity of the organic substance, the chemical hardness of iron (110) (0 eV), and the chemical hardness of the organic substance, successively.

Monte Carlo and molecular dynamics simulations

The adsorption of the Schiff base compound MPHCA on the Fe (110) surface was explored utilizing Monte Carlo simulations with the adsorption locator module in the Materials Studio software. Molecular dynamics simulations were conducted utilizing the Forcite model in Materials Studio 17. The simulations used the NVT ensemble with an Andersen thermostat, a 1.0 fs time step, and a duration of 20 ps at 298 K. The Fe (110) surface was cleaved along the (110) plane, and a five-layer slab was utilized. The iron (110) was expanded to a (10x10) supercell, and a 2.5 nm vacuum layer was constructed above the Fe (110) plane, which was filled with 100 water molecules and one inhibitor molecule. The COMPASS force field was employed to identify equilibrium configurations. The Ewald method was utilized to calculate electrostatic interactions with a high accuracy of 10^{-5}. The energy of adsorption (E_{ads}) of the examined compound on the iron surface was measured to understand the inhibitor's effectiveness. The radial distribution function (RDF) method assesses the chemical bonding between the MPHCA molecules and iron atoms.

Results and discussion

FTIR and ^{1}H NMR spectra

The elemental analysis of the synthesized MPHCA Schiff base substance was confirmed by FTIR (Figure 1A) and mass spectroscopy (Figure 1B).

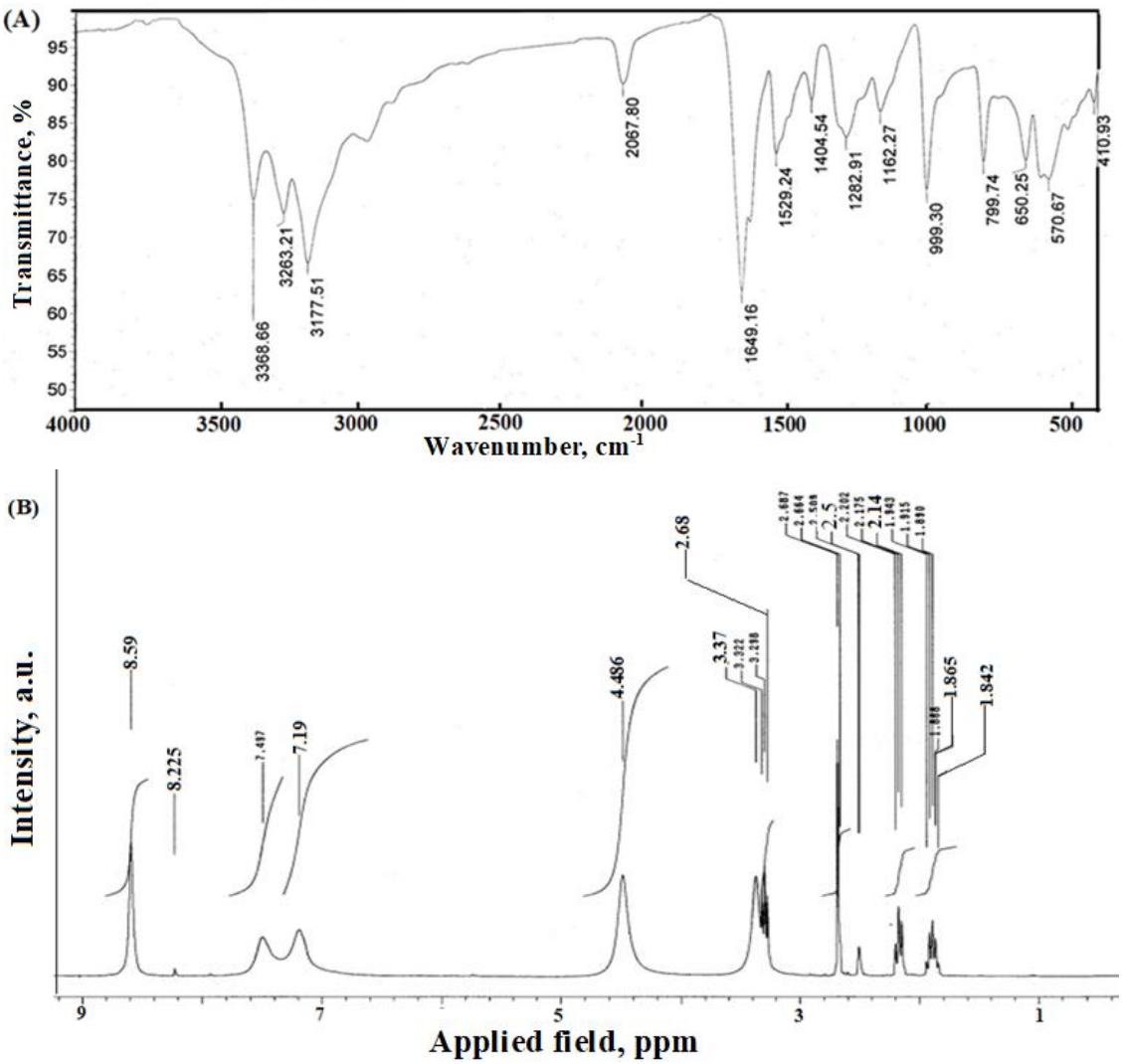

Figure 1. *(A) FTIR spectrum and (B) ^{1}H NMR spectrum of MPHCA Schiff base compound*

The structure of the pyrrole derivative was elucidated from spectral analysis. Thus, IR spectrum (Figure 1A) shows the stretching peaks for NH, CH_3, C=N, and C=S at 3360, 3177, 1649 and 1282 cm^{-1}, respectively.

The ^{1}H NMR spectrum of the prepared MPHCA compound is depicted in Figure 1B. The structure of the pyrrole derivative compound was deduced from spectral tools. Thus, proton NMR of the target showed signals at low applied field (downfield) at 8.59 and 7.19 ppm, for NCH_3 located at 3.37 ppm as a singlet signal, while cyclic CH's were observed as multiplets at 2.68, 2.50 and 2.14 ppm.

Mass loss investigation

The mass loss, ML, experiments were performed to examine the destructive influence of HCl on the examined metal surface in the absence and presence of the MPHCA compound, at various temperatures. The r_g values computed by Equation (1) were used to deduce the surface coverage and the inhibition efficiency (η_g), using Equations (2) and (3). In the absence of the MPHCA compound, the r_g is equal to 1.0494 mg cm^{-2} h^{-1}, which was decreased with increasing inhibitor concentration to reach 0.0243 mg cm^{-2} h^{-1}, at 5 mM of the MPHCA compound, at 25 °C. Figure 2A depicts the lowering in the r_g values with the addition of the MPHCA compound in the examined solution, at various temperatures. Figure 2B illustrates that the η_w / is increased with higher additions of the MPHCA compound and decreases as the temperature increases. The sigmoidal nature of such figures confirms the adsorption of the MPHCA molecules on the steel surface, which

will be explained later [26,28,29]. The lowering in the data of θ and η_w of the MPHCA compound with the temperature rise could confirm the escaping of some of the adsorbed MPHCA molecules from the metallic surface, entering the test solution. Such behaviour could be attributed to the physisorption nature of the adsorption process [30].

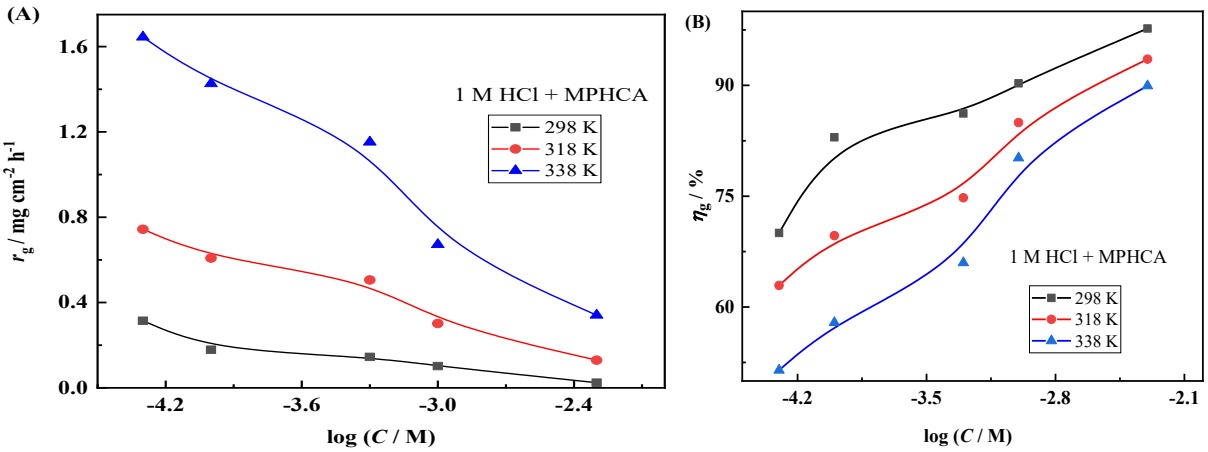

Figure 2. *(A) Variation of the rate of corrosion (r_g) of C-steel in 1.0 M HCl and (B) η_w with log C of MPHCA Schiff base compound at different temperatures*

Gasometric study

The vessel and experimental procedure for hydrogen evolution measurements have been described earlier [22,23]. The gasometric technique was utilized to investigate the inhibition behaviour of the MPHCA substance toward the destruction of carbon steel and hydrogen production in the acidic medium. The data shown in Figure 3A indicates that the volume of the produced H_2 (V_H) starts to increase faster after an incubation time (τ) that reaches 40 min in the free acid solution (1.0 M HCl), followed by a faster increase as time passes. The incubation time is elongated with more additions of the MPHCA compound (τ is increased from 100 to 165 min when the inhibitor concentration increases from 0.05 to 5 mM, at 25 °C), although it is reduced at higher temperatures. Higher concentrations of the MPHCA compound reduce the amount of the produced hydrogen (V_H). The accumulation of produced H_2 on the metallic surface after a certain time, τ, can illustrate the breakdown of the protective layer on the carbon steel surface due to the influence of Cl^- ions in the examined solutions [31,32]. The direct increase in the V_H with the immersion time could be attributed to the continuous destruction of the bare steel surface. It is noteworthy to see that the elongation (τ) at higher concentrations of the MPHCA compound could be explained by the enhancement of the inhibition process.

Figure 3B depicts the variation of the r_H values with the concentration of the MPHCA compound, at 298 and 318 K. Sigmoidal curves are obtained, a behaviour similar to that gained by the mass loss measurements, emphasizing adsorption of the MPHCA Schiff base molecules on the examined metal surface [31]. The values of corrosion parameters, as evaluated from H_2 gasometry and equations (4) and (5), are listed in Table 1. Although θ and η_H are increased with an increase in the MPHCA concentration, they are decreased with the temperature. Such behaviour confirms the escape of some of the adsorbed MPHCA species from the examined solution, indicating the physisorption process [33].

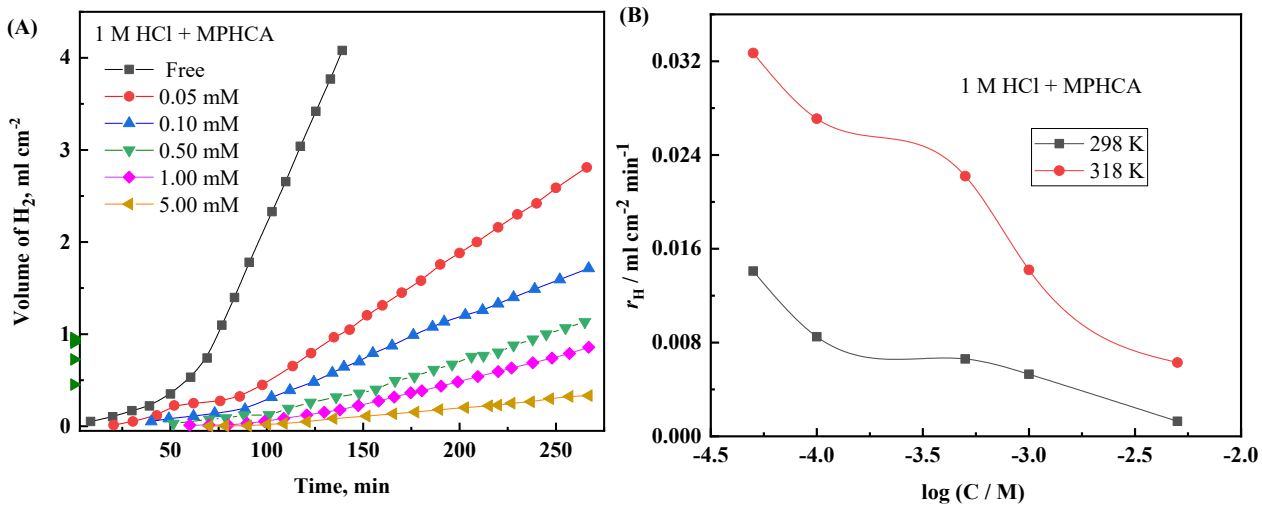

Figure 3. *(A)* V_H *vs. immersion time curves of C-steel in 1.0 M HCl without and with various concentrations of MPHCA, and (B) the rate of corrosion, expressed by the rate of hydrogen production* (r_H) *vs log* C *of MPHCA at 298 and 318 K*

Table 1. *The values of corrosion parameters deduced from gasometry data for different concentrations of the MPHCA inhibitor on C-steel immersed in 1.0 M HCl, at 298 and 318 K*

C / mM	$r_H \pm$ SD* / ml cm^{-2}min^{-1}		θ		η_H / %	
	298 K	318 K	298 K	318 K	298 K	318 K
0.00	0.04760 ± 0.0015	0.0871 ± 0.001				
0.05	0.01410 ± 0.0015	0.0327 + 0.001	0.704	0.625	70.4	62.5
0.10	0.00850 ± 0.0014	0.0271 ± 0.001	0.821	0.689	82.1	68.9
0.50	0.00660 ± 0.0012	0.0222 ± 0.001	0.861	0.745	86.1	74.5
1.00	0.00532 ± 0.0010	0.0142 ± 0.001	0.888	0.837	88.8	83.7
5.00	0.00128 ± 0.0010	0.0063 ± 0.001	0.954	0.928	95.4	92.8

*standard deviation

Potentiodynamic study

The potentiodynamic, PD, curves of the carbon steel in the aggressive (HCl) and inhibitive solutions (HCl mixed with MPHCA) are shown in Figure 4. Figure 4 suggests that the presence of the MPHCA does not show an effective influence on E_{corr} compared to the corrosive HCl solution. Such behaviour explains that the MPHCA Schiff base inhibitor retards the anodic dissolution of iron and cathodic reduction of H^+ ions. Here, the difference of E_{corr} in the corrosive and inhibitive solutions lies within ±21 mV, which confirms that the MPHCA compound attitudes as a mixed-type inhibitor [30]. The protection efficiency, η_p, of the MPHCA Schiff base inhibitor was deduced from the j_{corr} values in the aggressive HCl solution without and with the MPHCA inhibitor using Equation (6).

The various electrochemical corrosion factors, *i.e.* corrosion potential (E_{corr}) polarization resistance (R_p), corrosion current density, (j_{corr}), cathodic and anodic Tafel slopes (β_c and β_a), and inhibition efficiency (η_p) were calculated and tabulated in Table 2. The value of $j_{corr,}$ in the dilute HCl solution, is equal to 1.07 mA cm^{-2} and is reduced to 0.04 mA cm^{-2} in the presence of a 5 mM MPHCA inhibitor. The values β_a and β_c do not indicate a remarkable variation that is owing to the likeness in the mechanism of corrosion in the free acid and the inhibitive solutions [33].

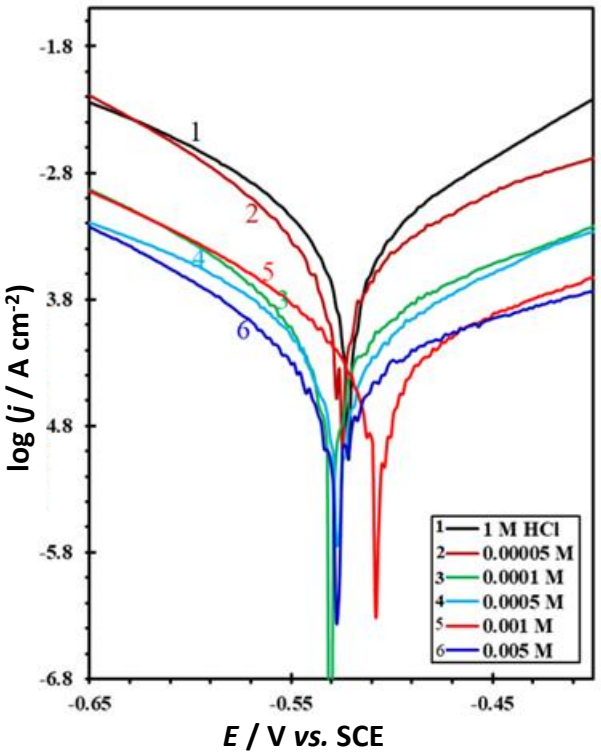

Figure 4. *The potentiodynamic polarization curves of C-steel in 1.0 M HCl solution, free of and mixed with various amounts of MPHCA inhibitor*

Table 2. *Potentiodynamic polarization parameters for C-steel in 1.0 M HCl, in the presence of different amounts of MPHCA inhibitor, at 298 K*

C / mM	E_{corr} / mV *vs.* SCE	$j_{corr} \pm$ SD* / mA cm^{-2}	β_a / mV dec^{-1}	β_c / mV dec^{-1}	R_p / Ω cm^2	η_p / %
0.00	-524	1.0697 ± 0.0015	153	-179	42	-
0.05	-504	0.2888 ± 0.0013	155	-174	158	73.00
0.10	-500	0.1821 ± 0.0011	166	-189	191	82.98
0.50	-503	0.1321 ± 0.0010	158	-167	204	87.65
1.00	-533	0.0923 ± 0.0009	162	-166	283	91.37
5.00	-522	0.0412 ± 0.0009	138	-148	450	96.15

*standard deviation

As seen in Table 2, η_p increases with the addition of the MPHCA inhibitor, resulting in a decrease in j_{corr}. Such behaviour can be illustrated by the shift of both the anodic and cathodic branches of the curves in Figure 4 toward lower values, which is attributed to a decrease in the rates of anodic Fe dissolution and cathodic H^+ ion reduction due to the inhibitory effect of the MPHCA inhibitor [14]. The presence of the MPHCA Schiff base compound in the corrosive acidic media increases the R_p value from 42 Ω cm^2 in the corrosive dilute hydrochloric acid solution to 450 Ω cm^2 when 5 mM of the MPHCA compound is mixed with the corrosive solution, proving the uniformity of the adsorbed protective layer formed by the adsorption process. The rise in the R_p and η_p values with more additions of the MPHCA inhibitor could indicate an increase in the thickness of the adsorbed film of MPHCA molecules on the investigated carbon steel surface [14].

EIS investigation

The EIS is considered a rapid non-destructive technique that is utilized to examine Nyquist curves of the investigated carbon steel in the aggressive acid solution, free of, and mixed with various amounts of MPHCA Schiff base inhibitor. Figure 5 shows that the EIS curves of the examined carbon steel surface have been highly modulated when the MPHCA Schiff base compound is mixed with the

corrosive acid solution. The Nyquist data can be explained *via* the electrical equivalent circuit represented in Figure 5 [33].

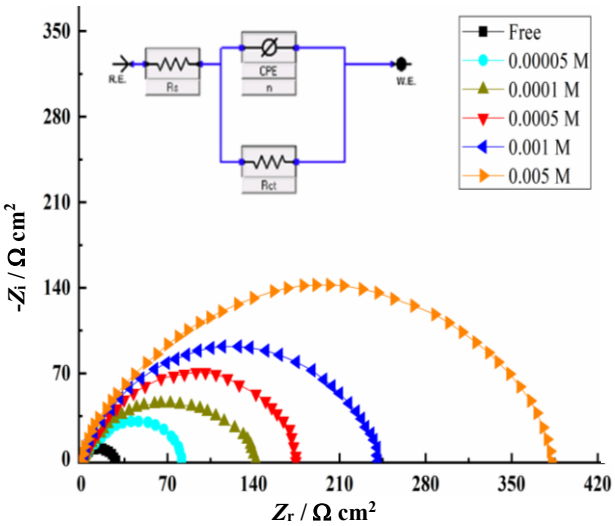

Figure 5. *Nyquist plots of C-steel in 1.0 M HCl solution, free of and mixed with various amounts of MPHCA inhibitor, at 25 °C; Inset: electrical equivalent circuit model used to fit the EIS data in the absence and presence of the MPHCA inhibitor*

The Nyquist plots depicted in Figure 5 show depressed and non-perfect semicircle capacitive loops formed in the absence and presence of the MPHCA compound in dilute HCl. The presence of capacitive loops in the examined frequency range for corrosive hydrochloric acid, both free and mixed with the MPHCA Schiff base inhibitor, indicates that the MPHCA Schiff base compound has a protective effect against the corrosion of the carbon steel surface. Such an effect proves that the inhibition mechanism is associated with the charge transfer between the carbon steel and the MPHCA Schiff base molecules [12,13]. Such inhibitive molecules act as interface inhibitors that can easily adsorb onto the corroded interface, forming a protective layer that reduces the destructive effect of HCl on the metallic surface [12]. The addition of the MPHCA inhibitor to the investigated solution progressively increases the diameter of the capacitive loop, indicating the formation of a protective film on the examined carbon steel that reduces the contact of the HCl solution with the surface.

Bode plots shown in Figure 6A are used to illustrate the inhibitory role of the MPHCA compound on the metallic surface against the destructive influence of HCl. The Bode impedance magnitude diagram reveals a capacitive zone at moderate frequencies and a resistive zone at the highest and lowest frequencies. The rise in the height of peaks of Bode phase plots at higher concentrations of the MPHCA Schiff base could be related to the presence of a passive film on the investigated metallic surface [13]. Such influence would raise the protection efficiency, η_I, of the MPHCA Schiff base molecules by increasing the concentration of the MPHCA Schiff base compound in the solution. Additionally, in Figure 6B, the phase angle shifts to less positive values with increasing concentrations of the MPHCA Schiff base inhibitor, confirming the formation of a protective layer of MPHCA molecules that hinders the approach of the acidic solution to the carbon steel surface [13].

Various electrochemical impedance parameters gained by impedance measurements, such as Y_0, R_s, R_{ct}, and n were deduced by analysing the obtained data and listed in Table 3, while η_I and C_{dl} values are computed using equations (9) and (10), respectively. The addition of the MPHCA Schiff base compound to the corrosive acid solution increases the R_{ct} values, which could indicate an increase in the ability of MPHCA molecules to be adsorbed on the carbon steel surface, thereby reducing the rate of metal destruction [19]. The values of the C_{dl} are reduced with the higher

concentrations of the MPHCA compound, which could be related to the increase in the thickness of the electrical double layer owing to the lowering in the metal destruction rate, confirming the adsorption of the MPHCA molecules on the carbon steel surface forming a protective layer [34].

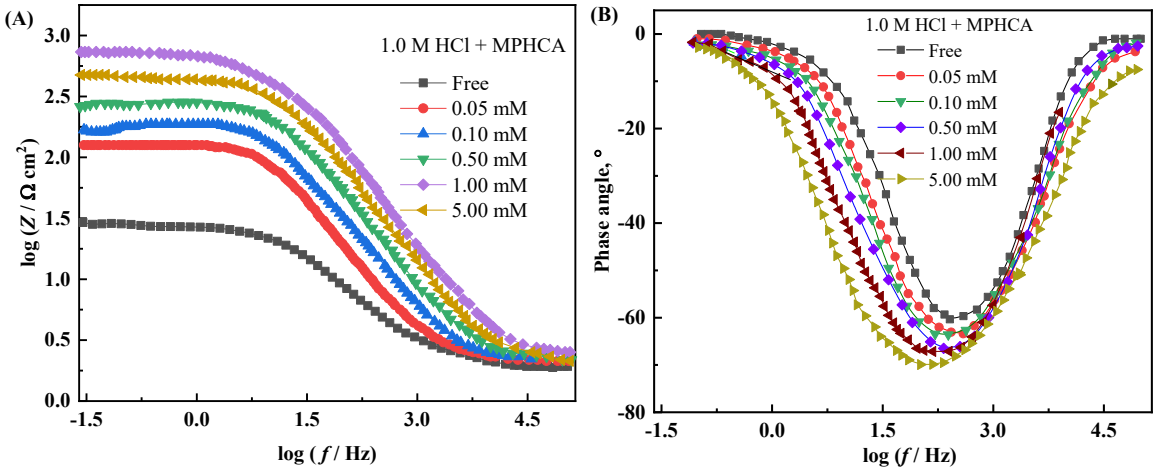

***Figure 6**. Bode magnitude (A) and phase angle (B) plots of C-steel in 1 M HCl solutions free of and mixed with various amounts of MPCHA inhibitor, at 25 °C*

***Table 3.** EIS data of C-steel in 1.0 M HCl, free of and mixed with various amounts of MPHCA Schiff base inhibitor, at 298 K*

C / mM	R_s / Ω cm^2	$Y_o \times 10^4$ / Ω^{-1}s^n cm^{-2}	n	R_{ct} + SD* / Ω cm^2	C_{dl} / μF cm^{-2}	η_I / %
0.00	839.7	0.2215	0.83	25.4 ± 0.009	280.4	-
0.05	2.40	0.803	0.85	82.4 ± 0.011	173	30.8
0.10	2.60	0.751	0.64	142 ± 0.016	141	82.1
0.50	2.30	0.598	0.80	174 ± 0.011	91.4	85.4
1.00	2.70	0.429	0.70	240 ± 0.011	52.9	89.4
5.00	4.60	0.391	0.70	385 ± 0.095	23.1	93.4

*standard deviation

Adsorption mechanism of MPHCA inhibitor

The inhibiting influence of the MPHCA inhibitor against the corrosion of carbon steel in hydrochloric acid solutions is supposed to be dependent on the adsorption of such organic species on the examined carbon steel surface. The adsorption of the inhibitor depends on several factors, including the chemical potential of the investigated metal, the chemical structure of the adsorbed molecules, and the temperature. The adsorption is increased with the increase in the number of adsorption sites and their electron density on the inhibiting molecules. The adsorption process is considered as a replacement process between the used MPHCA species and H_2O molecules that are already adsorbed on the metallic surface *via* the equilibrium reaction represented by Equation (14) [35]:

$$\text{MPHCA}_{(sol)} + z\text{H}_2\text{O}_{(ads)} \leftrightarrow \text{MPHCA}_{(ads)} + z\text{H}_2\text{O}_{(sol)} \quad (14)$$

where z represents the number of desorbed $H_2O_{(ads)}$ molecules replaced by one molecule of $MPHCA_{(ads)}$ inhibitor.

For approval, the general adsorption isotherms, including the Freundlich, Frumkin, Temkin, and Langmuir isotherms, were tested to obtain the most adequate isotherm for adsorption of $MPHCA_{(ads)}$ molecules on the surface of the utilized metal. It was found that the best-approved model is the Langmuir isotherm, which obeys Equation (15) [36,37]:

$$\frac{C}{\theta} = \frac{1}{K_{ads}} + C \quad (15)$$

where C is the equilibrium molarity of the utilized MPHCA Schiff base compound added to the corrosive solution (1.0 M HCl), θ is its surface coverage on the carbon steel, and K_{ads} is the adsorption-desorption equilibrium constant.

Equations for different adsorption isotherms and linear regression coefficients (r^2) are listed in Table 4. The values of θ were computed from gravimetric data by equation (2) and used to find the most suitable adsorption isotherm. According to the highest r^2, the superior model was found to be the Langmuir isotherm as the most appropriate adsorption model for MPHCA molecules on the investigated C-steel surface, which is explained by the formation of a monolayer of MPHCA molecules [22].

Table 4. *Various adsorption isotherms with obtained values of the regression coefficient,* R^2

Type	Equation	r^2
Temkin	$K_{ads} = e^{f\theta}$	0.856
Frundlich	$\theta = K_{ads} C^n$	0.843
Frumkin	$\theta / (1-\theta)\, e^{2f\theta} = K_{ads}C$	0.785
Langmuir	$C / \theta = K_{ads}C$	0.999

Figures 7A-C show the Langmuir isotherm plots, *i.e.* $C\theta^{-1}$ *vs.* C curves for the MPHCA Schiff base compound at 298, 318, and 338 K, respectively. Such plots depict straight-line relations with slopes very near 1, which confirms the Langmuir model with positive strong correlation coefficients ($R^2 \sim 1$).

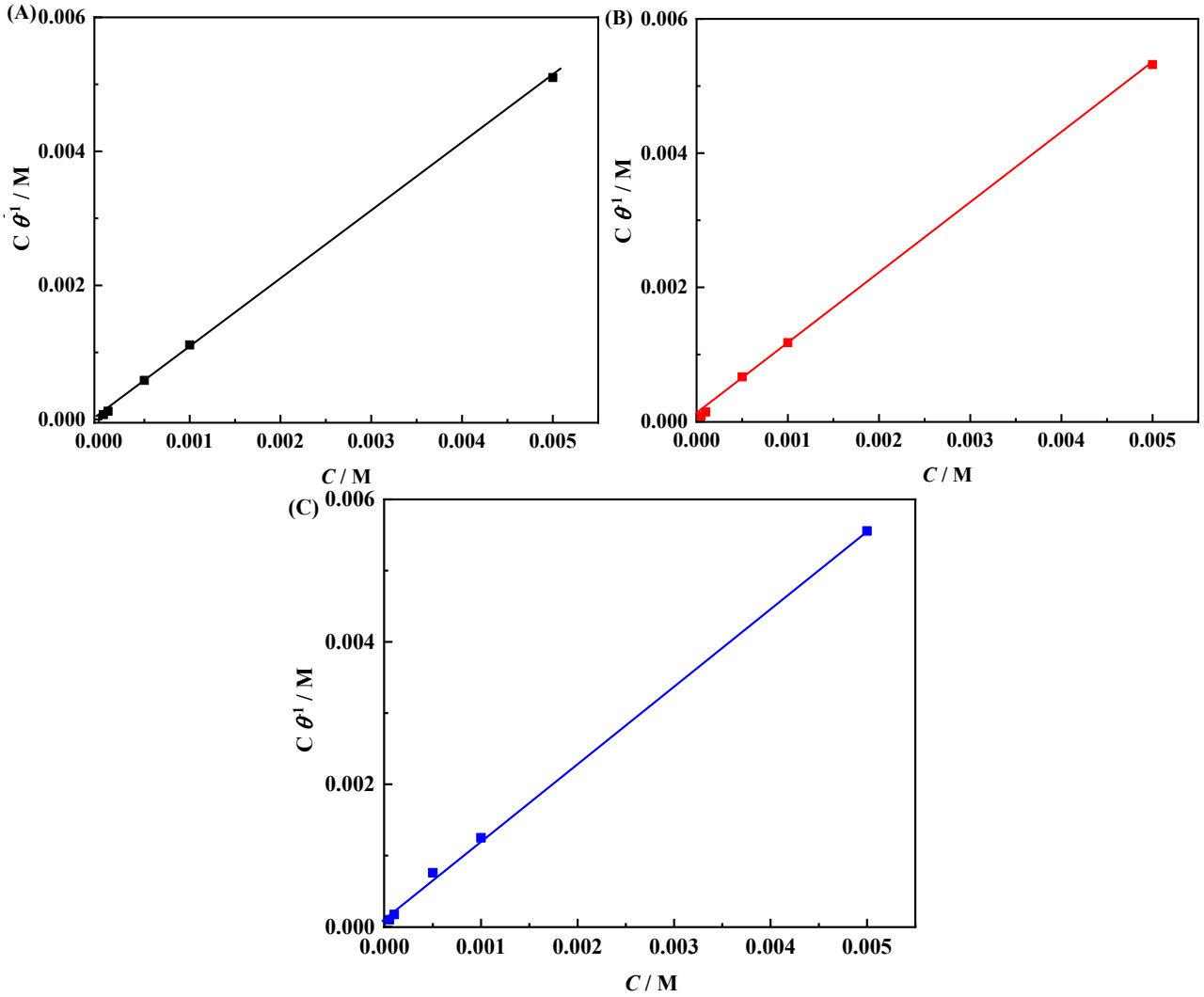

Figure 7*. Langmuir adsorption isotherms of the MPHCA inhibitor on the C-steel surface in 1.0 M HCl at various temperatures: (A)* T *=298 K, (B)* T *= 318 K and (C)* T *= 338 K*

The computed K_{ads} values are tabulated in Table 5. The decrease in the K_{ads} values with an increase in temperature (T) explains the decrease in the number of adsorbed MPHCA molecules from the corroded metal surface escaping into the investigated solution. The computed K_{ads} data listed in Table 5 were used to determine ΔG^{o}_{ads} *via* Equation (16) [25]:

$$\Delta G^{o}_{ads} = -RT\ (\ln K_{ads} + 4.0164) \quad (16)$$

The digit 4.016 represents the natural logarithm of the molar concentration of H_2O. The values ΔG^{o}_{ads} are listed in Table 5 and take values between -34.45 and -36.77 kJ mol^{-1}. The negative sign of the ΔG^{o}_{ads} could be attributed to the spontaneous nature of the adsorption of the MPHCA species on the examined carbon steel surface [38]. The computed values of ΔG^{o}_{ads} are lower than 20 kJ/mol and more than 40 kJ mol^{-1}, which could prove the probability of physical and chemisorption processes of the MPHCA molecules on the examined steel [17]. The lowering in the ΔG^{o}_{ads} values at higher temperatures would explain that protection from corrosion by the MPHCA Schiff base molecules is an endothermic process [39].

Table 5. *The values of* K_{ads}, ΔG^{o}_{ads}, ΔH^{o}_{ads} *and* ΔS^{o}_{ads}, *of adsorption of the MPHCA inhibitor on C-steel in 1.0 M HCl, at various temperatures*

T / K	K_{ads} / mM^{-1}	ΔG^{o}_{ads} / kJ mol^{-1}	ΔH^{o}_{ads}/ kJ mol^{-1}	ΔS^{o}_{ads} / J mol^{-1} K^{-1}
298	19.73	-34.45	-26.56	-173
318	12.57	-35.57		-166
338	8.68	-36.77		-160

The values of K_{ads} can be used to deduce the ΔH^{o}_{ads} value utilizing the Equation (17) [14]:

$$\ln K_{ads} = \left(\frac{-\Delta H^{o}_{ads}}{RT} \right) + \text{constant} \quad (17)$$

Figure 8 depicts ln K_{ads} values *vs.* T^{-1} to produce a straight-line plot. The slope of such a figure can be used to deduce the ΔH^{o}_{ads} value as listed in Table 5. The negative sign of the ΔH^{o}_{ads} explains that the adsorption of MPHCA Schiff base molecules is exothermic [14]. This behaviour confirms that the decrease in the η values at high temperatures supports the desorption process. A chemisorption process could be attained if the ΔH^{o}_{ads} values exceed 40 kJ mol^{-1} and can approach 400 kJ mol^{-1}. Here, the ΔH^{o}_{ads} = -26.56 kJ mol^{-1}, which affords the electrostatic adsorption of the MPHCA molecules on the investigated metal.

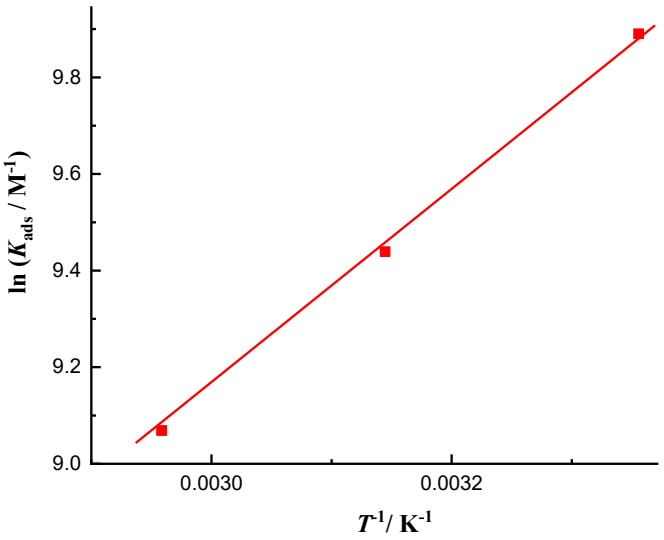

Figure 8. *Vant's Hoff plot (ln* K_{ads} vs. T^{-1}*) for the corrosion of C-steel in 1.0 M HCl in the presence of MPHCA inhibitor*

The standard entropy, ΔS^{o}_{ads} can be calculated from Equation (18) [13]:

$$\Delta G^{o}_{ads} = \Delta H^{o}_{ads} - T\Delta S^{o}_{ads} \quad (18)$$

The computed ΔS^{o}_{ads} listed in Table 5 have negative values that become less negative with the rise in temperature, confirming the adsorption of MPHCA Schiff base molecules on the investigated metal surface.

Temperature study

The importance of temperature lies in deducing the activation energy (E_a) that accompanies the corrosion process through the application of the Arrhenius equation. The r_g values computed by the mass loss method in the corrosive and inhibitive solutions at different temperatures (T) were utilized to verify the relation between the r_g values and T *via* Equation (19)[14]:

$$\log r_g = \left(\frac{-E_a}{2.303RT}\right) + \text{constant} \quad (19)$$

where R is the gas constant.

Figure 9A shows the variation of such relation for the carbon steel in the aggressive media (1.0 M HCl), free of and mixed with various concentrations of the MPHCA. This figure shows linear segments with slopes very near 1, which supports the implementation of the Arrhenius equation. The computed E_a values are tabulated in Table 6. The higher values of the E_a gained in the presence of MPHCA compound could suggest the physisorption of the MPHCA Schiff base compound on the examined metal [39-41].

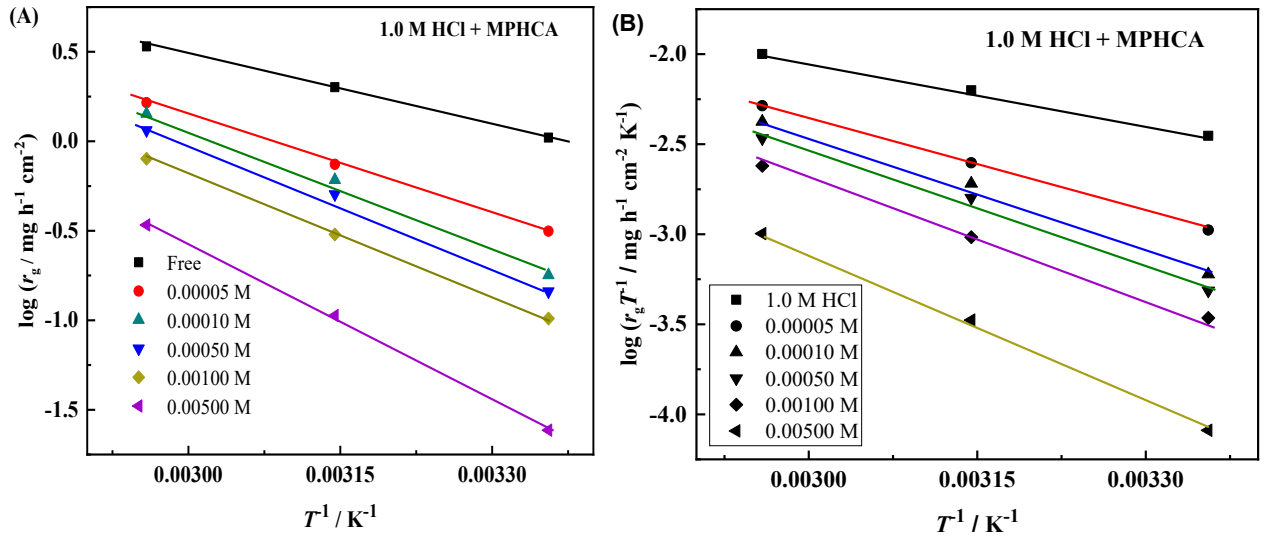

***Figure 9**. Arrhenius (A) and transition state plots (B) for different amounts of MPHCA inhibitor on C-steel in 1.0 M HCl*

The transition state equation is utilized to compute the ΔS^* and ΔH^* values for the corrosive and inhibitive solutions containing the MPHCA Schiff base using Equation (20) [26,39]:

$$\log(r_g T^{-1}) = \log\left(\frac{R}{N_A h}\right) + \left(\frac{\Delta S^*}{2.303R}\right) - \left(\frac{\Delta H^*}{2.303RT}\right) \quad (20)$$

where h and N_A are Planck's and Avogadro's constants, respectively. The plots of Figure 9B confirm the transition state equation by representing the variation of the log ($r_g T^{-1}$) with T^{-1} for corrosive HCl solutions free of and mixed with MPHCA to give straight line relations with regression coefficients very near to one. The calculated ΔH^* values are tabulated in Table 6. The computed value of ΔH^* with a positive sign could confirm the endothermic nature [32,40]. The ΔS^* are calculated to

be -171 J mol^{-1} K^{-1} with inhibitor-free acid solutions and vary between -143 to -99 J mol^{-1} K in the inhibitive solutions, relying on the amounts of MPHCA inhibitor in the solution. The negative values of ΔS^* for all concentrations of MPHCA could confirm the constancy of the inhibitor-formed film that adsorbs on the examined carbon steel surface [26]. The rise in the value of ΔS^* with higher amounts of the MPHCA compound would explain that the activated complex in the rate-determining process indicates an association rather than dissociation [42-47].

Table 6. *Activation thermodynamic parameters for C-steel in 1 M HCl solutions free of and mixed with various amounts of the MPHCA inhibitor*

C_{MPBA} / M	E_a / kJ mol^{-1}	ΔH^*_{ads} / kJ mol^{-1}	ΔS^*_{ads} / J mol^{-1} K^{-1}
Free	24.56	21.92	-171
0.05	34.62	33.29	-143
0.10	43.59	40.95	-122
0.50	43.64	40.90	-123
1.00	43.10	4074	-127
5.00	55.37	52.73	-99

Surface study

The surface morphology of the samples was examined under SEM and by EDS analysis. Figures 10 and 11 display the SEM images and EDS results of various electrodes of carbon steel samples.

The surface morphology of the dry steel sample, before immersion in the aggressive or inhibitive solution, is shown in Figure 10A. The morphology of the surface of such a sample appears to be smooth without indication of any destruction; only scratching and continuous lines appear due to the abrading process. The second sample of the C-steel was immersed in 250 mL of the aggressive 1.0 M HCl solution for four hours, followed by washing and drying, and then investigated under SEM. The surface morphology of a corroded C-steel sample is shown in Figure 10B, which depicts a damaged surface surrounded by corrosion products resulting from the corrosive acid's effect, which tends to dissolve iron atoms from the carbon steel. Figure 10C displays the surface micrograph of the examined metallic surface after being picked up from the inhibitive solution that contains 0.005 M MPHCA in 1.0 M HCl solution. This micrograph shows a less damaged metallic surface due to corrosion. The presence of MPHCA inhibitor retards the destructive effect of hydrochloric acid through adsorption process.

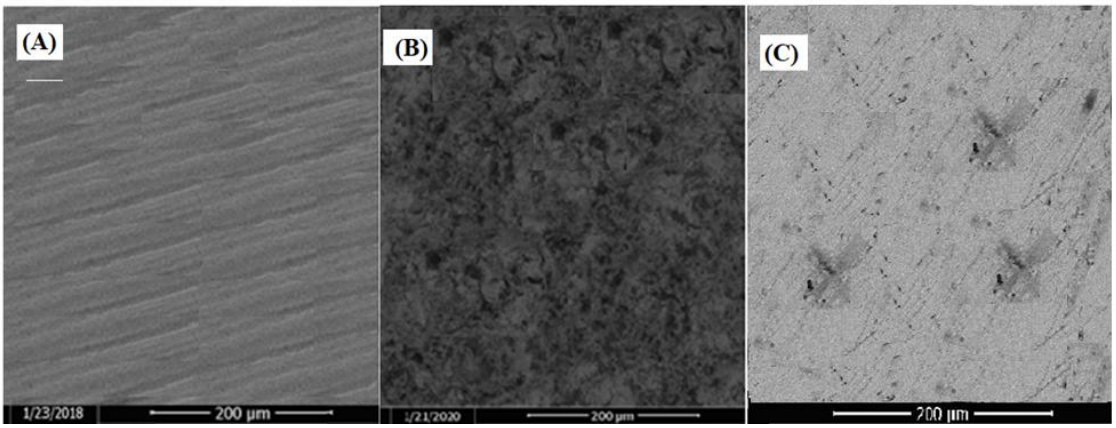

Figure 10. *SEM micrographs of C-steel before (A), and after immersion in 1 M HCl, free of (B), and mixed with 5 mM MPHCA inhibitor (C)*

The data of the EDS analysis could confirm the destructive and inhibitive effects of HCl and the MPHCA inhibitor *via* the chemical composition of the formed protective film on the metallic

surfaces. Figure 11A depicts the EDS spectrum with some characteristic peaks for the polished C-steel with an iron composition of 98.75 %.

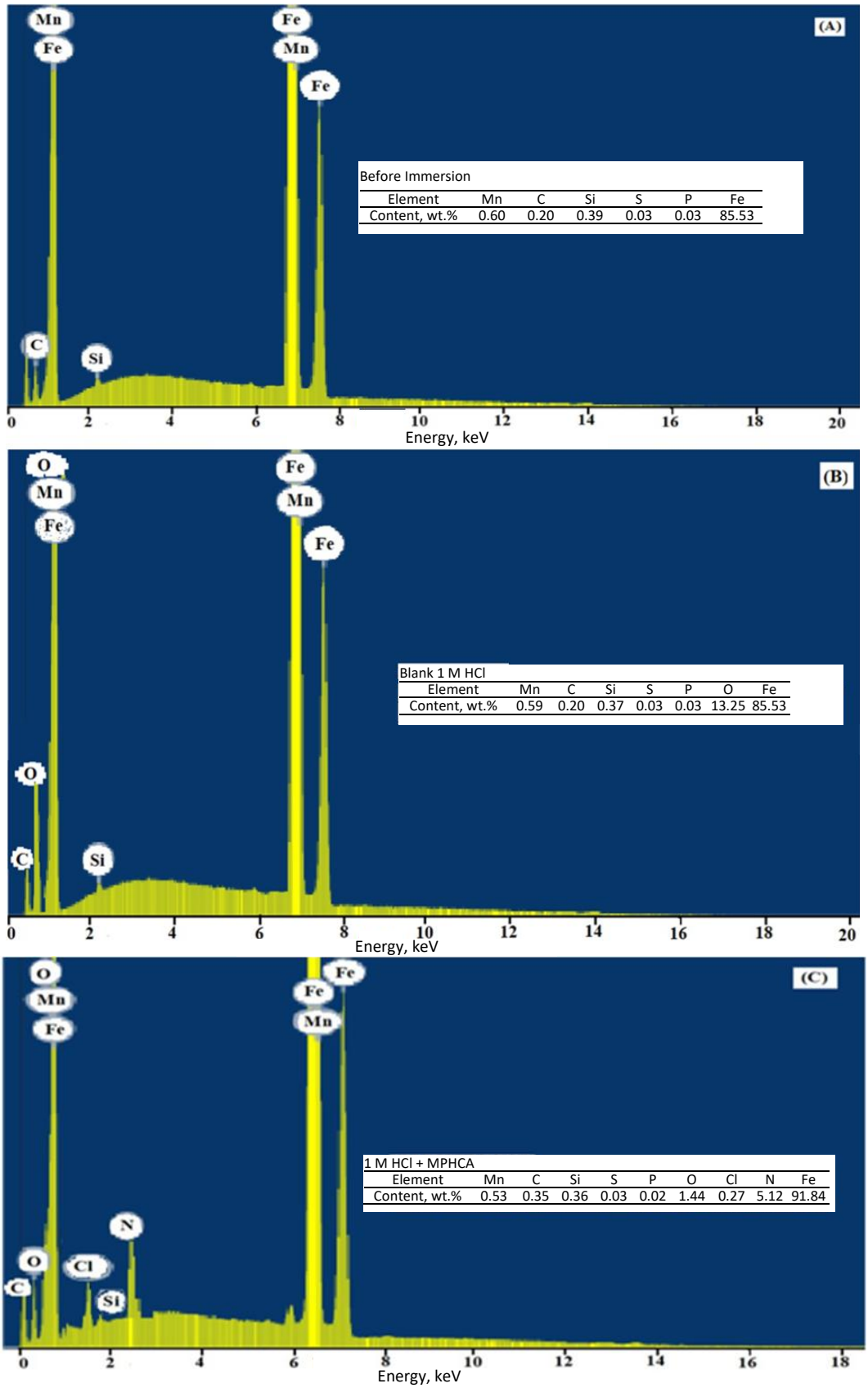

***Figure 11**. EDX spectra of C-steel before (A), and after immersion in 1 M HCl, free of (B) and mixed with 5 mM MPHCA inhibitor (C)*

The EDS spectrum in the case of the C-steel sample immersed in 1 M HCl solution free of inhibitor (Figure 11 B) showed a decrease in the intensity of the Fe peak owing to the dissolution of Fe during the corrosion process (Fe content = 85.53 %). In the presence of 0.005 M of MPHCA inhibitor, the surface of the C-steel sample was greatly improved due to the formation of a protective film of the organic inhibitive molecules, as indicated by the decrease of the iron band with Fe content reaching 91.84 %. Figure 11C indicates that the protective film formed was strongly adherent to the surface, resulting in a high degree of inhibition efficiency.

DFT computations

The MPHCA inhibitor was optimized in an aqueous medium using the CPCM model. The optimized geometry presented in Figure 12A supplies valuable insights into the structure and potential characteristics of the investigated molecule. The MPHCA is characterized by the bond lengths between C-N and C-C for a single bond around 0.14 and 0.15 nm, respectively. The bond angles between C3-N11-C4 are close to the expected 113.43° for sp^3 hybridized C and N atoms. The negative dihedral angle (-179.26°) between N11-C4-N16-N17 in the MPHCA inhibitor suggests some degree of conjugation.

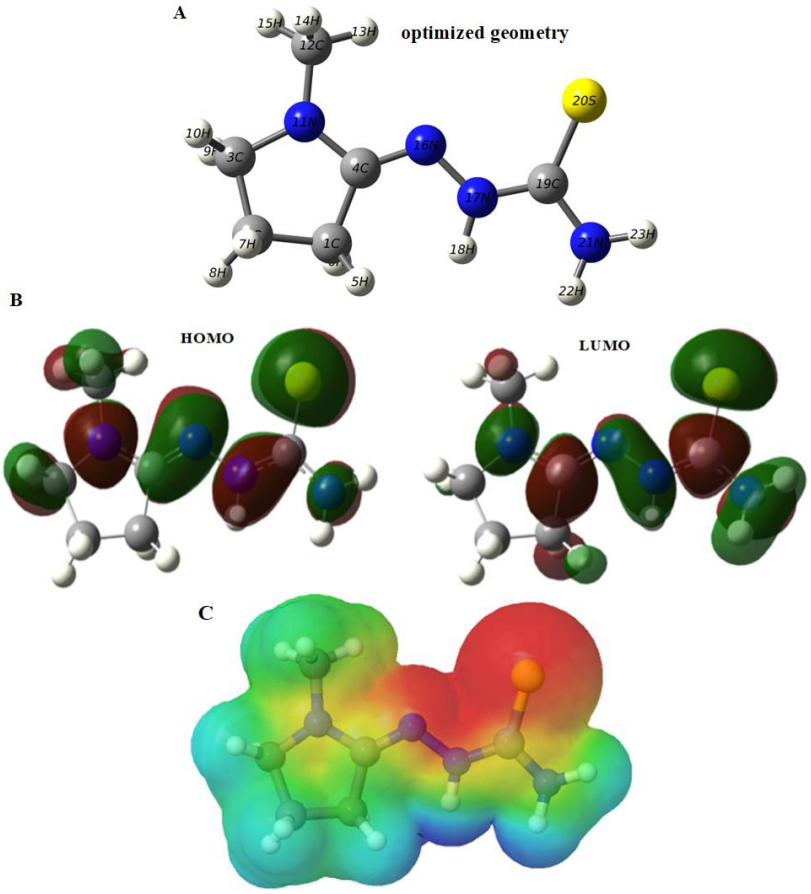

Figure 12. *The optimized geometry (A), frontier orbital, FMO (B), and the electrostatic potential map (C) of the MPHCA Schiff base inhibitor*

The frontier orbital theory includes HOMO and LUMO, aiding in identifying the adsorption sites of inhibitive organic molecules during interactions with metal surfaces. The inhibitors likely function as electron donors to the metal surface, emphasizing the importance of HOMO electron density distribution. LUMO shows the electron-accepting areas of the organic compounds during their interaction with a metal surface. Additionally, the energy gap (ΔE) between HOMO and LUMO levels is a key aspect to consider when assessing inhibitor molecules. The 3D plots of frontier molecular

orbitals for the MPHCA inhibitor are depicted in Figure 12 B, which shows that HOMO and LUMO orbital distributions are the same for the MPHCA molecule.

The molecular electrostatic potential (ESP) serves as a valuable tool for identifying reactive sites for nucleophilic and electrophilic attacks. ESP is linked to a molecule's polarity, dipole moment, and charge distribution. ESP maps of the MPHCA inhibitor can be seen in Figure 12C. The maps use yellow and red colours to represent negative potential, while blue and green signify positive and neutral potential, respectively. Highly electronegative regions are found on the nitrogen and sulphur atoms in the MPHCA inhibitor. In contrast, positive potentials are found in the methyl pyrrolidine group.

These observations highlight that the electron-rich regions on these molecules make them preferred sites for adsorption on metal surfaces. This is important for understanding how these inhibitors interact with metal surfaces and their effectiveness in preventing corrosion.

The electron-rich sites on MPHCA enhance its ability to interact with the metal surface, forming a protective layer. This selective adsorption mechanism, guided by the ESP map, is crucial for maximizing the inhibitor efficiency and ensuring comprehensive protection against corrosion. The identification of nucleophilic and electrophilic sites is crucial for predicting how inhibitors will behave during the corrosion inhibition process.

The negative sign of E_{HOMO} (-5.31 eV) is owing to the association with the power of the inhibitive molecule [48,49], which explains the inclination of the inhibitive species to contribute electrons to the acceptor molecule E_{LUMO}. Concerning the energy gap, ΔE = 5.05 eV, a lower value will reflect the higher protection ability due to the higher reactivity of such a molecule. This can be attributed to the low energy needed to repel an electron from the last occupied orbital [50,51]. This energy gap facilitates the transfer of electrons between the inhibitor and the metal, promoting adsorption and forming a protective layer. Quantitative comparison between theoretical and experimental inhibition efficiencies further validates these findings. Theoretical calculations for the inhibition efficiency of MPHCA, derived using DFT parameters such as ΔE and global descriptors, show a strong correlation with experimental efficiencies exceeding 95 % at a concentration of 5.0 mM. Such consistency confirms the reliability of computational methods in predicting and explaining the mechanisms of corrosion inhibition.

Lewis-based molecules, known for their ability to donate and accept electrons, are particularly effective at corrosion prevention. Softer molecules outperform harder molecules due to their enhanced reactivity and capacity to form stable interactions with metal surfaces. This allows softer molecules to create protective layers, improving corrosion resistance [52]. In this study, the MPHCA inhibitor with lower hardness and higher softness is found to be an effective inhibitor for corrosion prevention. The electron transfer fraction (ΔN =0.4 eV) measures the transfer of electrons from a molecule to a metal when $\Delta N > 0$, and from a metal to a molecule when $\Delta N < 0$ [51]. The positive value of ΔN suggests that electrons are transferred from the metal to the inhibitor molecule. The ΔE and ΔN parameters are critical in predicting the performance of corrosion inhibitors like MPHCA. The ΔE for MPHCA (5.05 eV) signifies a balanced combination of molecular stability and reactivity, facilitating effective electron donation and acceptance during adsorption on the carbon steel surface. Similarly, the ΔN parameter quantifies the fraction of electrons transferred between the inhibitor and the metal surface. A positive ΔN value indicates that the inhibitor donates electrons to the metal, promoting adsorption and the formation of a protective barrier [14].

To understand how a molecule interacts with specific sites on a metal surface, the molecule should ideally target the active corrosion sites. The Fukui function helps provide insight into a molecule's local reactivity by showing how its electron density changes when it either gains or loses

an electron. This function is split into two types: f^+ for nucleophilic attack and f^- for electrophilic attack, which can be computed by Equations (21) and (22)

$$f^+ = q(N) - q(N + 1) \quad (21)$$

$$f^- = q(N - 1) - q(N) \quad (22)$$

where $q(N)$, $q(N + 1)$, $q(N - 1)$ are the charges of atoms for N, N+1, and N-1 electron systems, successively. A higher f^+ value for a given atom suggests a preference for a nucleophilic attack, indicating the atom is more likely to donate electrons. Conversely, higher f^- values point to a preference for electrophilic attack, suggesting the atom is more likely to accept electrons. This differentiation helps determine how the inhibitor interacts with the metal surface, influencing its efficacy in corrosion prevention. MPHCA Schiff base inhibitor molecule shows that the sites for nucleophilic attack are C (19) and S (20), while the sites for electrophilic attack are N (16) and S (20).

Monte Carlo and molecular dynamics simulations

The effectiveness of the MPHCA Schiff base compound in preventing corrosion through adsorption on Fe (110) can be obtained from the results of the Monte Carlo simulation. This simulation provides energy values for the system, including the iron (110) surface, Schiff base species, and 100 molecules of H_2O solvent. The equilibrium configuration of the adsorbed Schiff base species on the iron (110) surface, shown in Figure 13, manifests that the MPHCA compound is aligned parallel to the Fe surface.

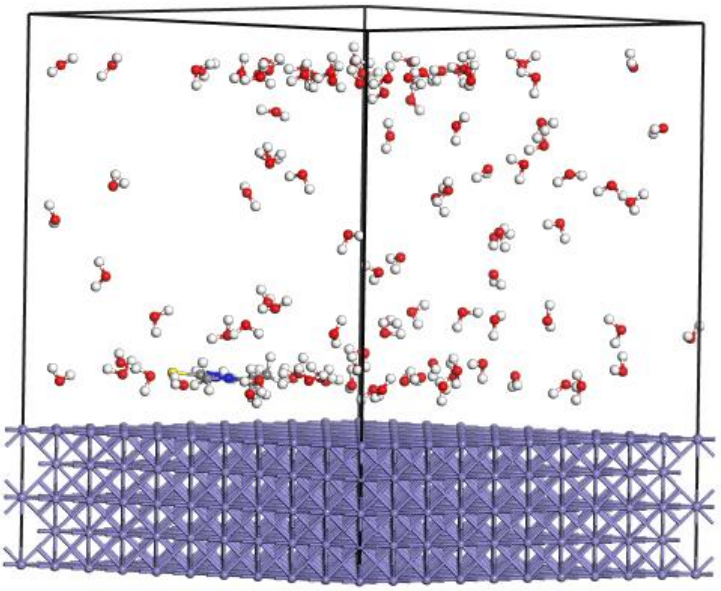

***Figure 13**. Adsorption of the MPHCA inhibitor on the Fe (110) surface*

MPHCA inhibitor exhibits the most negative adsorption energy (1764.9 kJ mol^{-1}), indicating the highest interaction with the Fe surface.

The radial distribution function (RDF) is employed to analyse bonding characteristics, depicted by the RDF (radial distribution function), or $g(r)$. Peaks at 1 and 0.35 nm signify chemisorption, indicating a strong chemical bond between the MPHCA Schiff base molecules and the Fe atoms. In contrast, peaks beyond 0.35 nm suggest physisorption, representing weaker physical interactions. Figure 14 displays the first noticeable peak at less than 0.35 nm, pointing to the dominance of chemical bonds between the MPHCA molecules and Fe atoms.

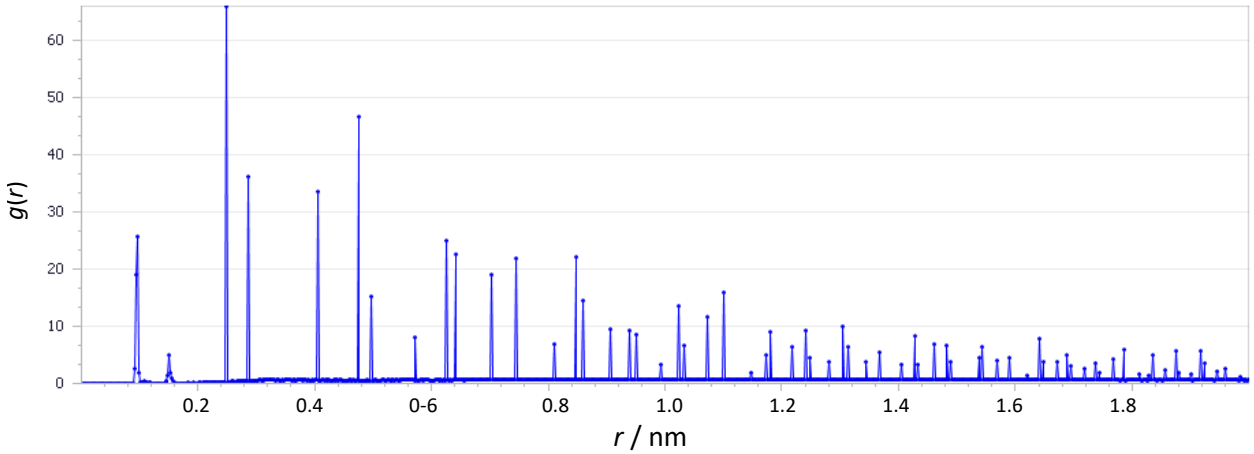

***Figure 14**. Radial distribution function g(r) analyses for MPHCA inhibitor on the Fe (110) surface*

The stability of the parallel alignment of MPHCA on the Fe (110) surface is supported by molecular dynamics (MD) simulations, which reveal that the inhibitor remains consistently adsorbed over time due to strong interactions between its electron-rich regions and the metal surface. This stability is further corroborated by the high adsorption energy (-1764.9 kJ mol^{-1}), indicating robust adsorption. Such results align with experimental findings, particularly the high surface coverage (θ) values and the significant inhibition efficiencies observed, confirming the reliability of the computational predictions. The radial distribution function (RDF) analysis provides additional insights into the nature of the adsorption process. The peaks at distances less than 0.35 nm signify chemisorption, as they indicate strong chemical bonding between the MPHCA molecule and the Fe atoms. In contrast, peaks at greater distances represent weaker physical interactions (physisorption). The dominant chemisorption observed in the RDF analysis is consistent with the high adsorption energy and the experimental observation of stable and effective inhibitor layers on the carbon steel surface. This comprehensive understanding of the adsorption mechanism underscores the synergistic relationship between simulation and experimental data. Additional peaks beyond 0.35 nm highlight the presence of physical interactions. The data support the comprehensive adsorption of the examined MPHCA Schiff base compound on the investigated carbon steel surface. The highest adsorption energy and a greater degree of chemisorption demonstrate the superior corrosion inhibition properties of the MPHCA inhibitor**.** Finally, the data of the MD and RDF techniques are strongly proportional to the experimental data.

Conclusions

The MPHCA inhibitor was synthesized and structurally confirmed by the FTIR and mass spectroscopy measurements.

- Such a compound is a mixed kind mitigator that retards the metal destruction and hydrogen generation in dilute HCl solutions.
- The data of the rate of corrosion (r_{corr}), surface coverage, (θ) and the inhibition efficiency (η) gained by various experimental techniques are consistent with the theoretical calculations.
- The r_{corr}, θ and η values were found to rely on the MPHCA amount and temperature.
- The protection process is based on the adsorption of the MPHCA species on the carbon steel surface according to Langmuir's isotherm.
- Lowering the surface coverage values and percent inhibition with temperature could approve the physisorption of the MPHCA species on the carbon steel surface.

- The higher values of K_{ads} could indicate the strong adsorption of the MPHCA on the carbon steel surface.
- The minus sign of the $\Delta G°_{ads}$ manifests the spontaneous nature of the adsorption of the MPHCA molecules on the carbon steel surface.
- The adsorption of MPHCA Schiff base molecules on the examined carbon steel surface can be explained by the chemisorption mechanism.
- The data of the quantum study proved that the adsorption of the MPHCA is consistent with the data of the experimental measurements.
- The study might provide advice on using the MPHCA compound as a good inhibitor for the corrosion of steel in petroleum fields.

Acknowledgements: *The authors extend their appreciation to the Deanship of Scientific Research at Northern Border University, Arar, KSA, for funding this research work through the project number "NBU-FFR-2025-144-02." The authors express their gratitude to Princess Nourah bint Abdulrahman University Researcher for supporting project number (PNURSP2025R53) - Princess Nourah bint Abdulrahman University, Riyadh, Saudi Arabia.*

Competing interest*: The authors declare no competing financial interest.*

References

[1] A. A. Farag, M. A. Migahed, A. M. Al-Sabagh, Adsorption and inhibition behavior of a novel Schiff base on carbon steel corrosion in acid media, *Egyptian Journal of Petroleum* **24** (2015) 307-315. https://doi.org/10.1016/j.ejpe.2015.07.001

[2] M. Finšgar, J. Jackson, Application of corrosion inhibitors for steels in acidic media for the oil and gas industry, *Corrosion Science* **86** (2014) 17-41. https://doi.org/10.1016/j.corsci.2014.04.044

[3] M. A. Deyab, M. M. Abdeen, M. Hussien, I. E. El-Sayed, A. Galhoum, O. A. A. El-Shamy, M. Abd Elfattah, Novel corrosion inhibitor for carbon steel in acidic solutions based on α-aminophosphonate (chemical, electrochemical, and quantum studies, *Molecules* **28** (2023) 4962. https://doi.org/10.3390/molecules28134962

[4] K. M. Shwetha, B. M. Praveen, B. K. Devendra, A review on corrosion inhibitors: Types, mechanisms, electrochemical analysis, corrosion rate, and efficiency of corrosion inhibitors on mild steel in an acidic environment, *Results in Surfaces and Interfaces* **16** (2024) 100258. https://doi.org/10.1016/j.rsurfi.2024.100258

[5] N. Betti, A. A. Al-Amiery, W. K. Al-Azzawi, W .N. R. Wan Isahak, Corrosion inhibition properties of Schiff base derivative against mild steel in HCl environment complemented with DFT investigations, *Scientific Reports* **13** (2023) 8979. https://doi.org/10.1038/s41598-023-36064-w

[6] A. Recherache, F. Benghanem, L. Toukal, N. Bounedjar, M. Foudia, B. Abebe, M. W. Alam, Electrochemical, quantum chemical, and thermodynamic investigation of a Schiff base corrosion inhibitor for XC70 steel, *Scientific Reports* **15** (2025) 19350. https://doi.org/10.1038/s41598-025-04051-y

[7] T. Mohamed, T. Mustapha, Z. Hassan, J. Charafeddine, B. Fouad, Z. Abdelkader, B. Fouad, *Citrullus colocynthis* fruit extract as effective eco-frindely corrosion inhibitor in a hydrochloric acid pickling medium for carbon steel by using both experimental and theoretical studies, *Environmental Science and Pollution Research* **31** (2024) 43757-43780. https://doi.org/10.1007/s11356-024-34055-6

[8] P. Du, S. Deng, G. Du, D. Shao, D. Xu, Xi. Li, Synergistic inhibition effect of *Mikania micrantha* extract with potassium iodide on the corrosion of cold rolled steel in methanesulfonic acid solution, *Corrosion Science* **220** (2023) 111296. https://doi.org/10.1016/j.corsci.2023.111296

[9] S. Y. Peng, Z. N. Jiang, Y. R. Li, C. F. Dong, H. F. Liu, G. A. Zhang, A new exceptional imidazoline derivative corrosion inhibitor for carbon steel in supercritical CO_2 environment, *Corrosion Science* **245** (2025) 112663. https://doi.org/10.1016/j.corsci.2024.112663

[10] J. Pi, M. Chen, T. Chen, Q. Wang, S. Cheng, C. Fu, Corrosion inhibition effect of 1-phenyl-5-mercaptotetrazole on nickel-aluminum bronze in seawater: A combined experimental and theoretical study, *Colloids and Surfaces A* **666** (2023) 131354. https://doi.org/10.1016/j.colsurfa.2023.131354

[11] B. Fan, H. Zhu, H. Li, H. Tian, B. Yang, Penetration of imidazoline derivatives through deposited scale for inhibiting the under-deposit corrosion of pipeline steel, *Corrosion Science* **235** (2024) 112209. https://doi.org/10.1016/j.corsci.2024.112209

[12] X. Wang, J. Yang, X. Chen, 2-Benzylsulfanyl-1H-benzimidazole and its mixture as highly efficient corrosion inhibitors for carbon steel under dynamic supercritical CO_2 flow conditions, *Corrosion Science* **235** (2024) 112170. https://doi.org/10.1016/j.corsci.2024.112170

[13] N. Z. Nor Hashim, E. H. Anouar, K. Kassim, H. M. Zaki, A. I. Alharthi, Z. Embong, XPS, and DFT investigations of corrosion inhibition of substituted benzylidene Schiff bases on mild steel in hydrochloric acid, *Applied Surface Science* **476** (2019) 861-877. https://doi.org/10.1016/j.apsusc.2019.01.149

[14] W. Zhang, H.-Jing Li, M. Wang, Li-Juan Wang, Ai-Han Zhang, Yan-Chao Wu, Highly effective inhibition of mild steel corrosion in HCl solution by using pyrido[1,2-a]benzimidazoles, *New Journal of Chemistry* **43** (2019) 413-426. https://doi.org/10.1039/C8NJ04028A

[15] G. Wei, S. Deng, Y. Qiang, Y. Zhang, X. Li, Halogenated pyrimidines as promising inhibitors for cold rolled steel in HCl and H2SO4 media: Experiments and theoretical calculations, *Corrosion Science* **246** (2025) 112724. https://doi.org/10.1016/j.corsci. 2025.112724

[16] H. Ferkous, S. Djellali, R. Sahraoui, H. Behloul, K. Saoud, A. Çukurovali, Corrosion inhibition of mild steel by 2-(2-methoxybenzylidene) hydrazine-1-carbothioamide in hydrochloric acid solution: Experimental measurements and quantum chemical calculations, *Journal of Molecular Liquids* **307** (2020) 112957. https://doi.org/10.1016/j.molliq.2020.112957

[17] F. Boudjellal, H. B. Ouici, A. Guendouzi, O. Benali, A. Sehm, Experimental and theoretical approach to the corrosion inhibition of mild steel in acid medium by a newly synthesized pyrazole carbothioamide heterocycle, *Journal of Molecular Structure* **1199** (2020) 127051. https://doi.org/10.1016/j.molstruc.2019.127051

[18] N. Mouats, S. Djellali, H. Ferkous, A. Sedik, A. Delimi, A. Boublia, K. O. Rachedi, M. Berredjem, A. Çukurovali, M. Alam, B. Ernsti, Y. Benguerba, Comprehensive investigation of the adsorption, corrosion inhibitory properties, and quantum calculations for 2-(2,4,5-trimethoxybenzylidene) hydrazine carbothioamide in mitigating corrosion of XC38 carbon steel under HCl environment, *ACS Omega* **9** (2024) 27945-27962. https://doi.org/10.1021/acsomega.3c10240

[19] A. Ashraf, N. Riaz, S. Muzaffar, M. Atif, B. Bashi, Investigating the potential of 1,2,4-triazoles as corrosion inhibitors for copper and steel: A comprehensive review, *Next Research* **1** (2024) 100033. https://doi.org/10.1016/j.nexres.2024.100033

[20] D. I. Udunwa, O. D. Onukwuli, S. C. Nwanonenyi, C. B. Ezekannagha, Novel imidazole-based ionic liquid as anti-corrosion additive for aluminum alloy: Combined experimental, DFT/MD simulation and soft computing approach, *Applied Surface Science Advances* **19** (2024) 100578. https://doi.org/10.1016/j.apsadv.2024.100578

[21] Y. Zhu, M. L. Free, R. Woollam, W. Durnie, A review of surfactants as corrosion inhibitors and associated modeling, *Progress in Materials Science* **90** (2017) 159-223. https://doi.org/10.1016/j.pmatsci.2017.07.006

[22] E.A. Noor, A.H. Al-Moubaraki, Corrosion behavior of mild steel in hydrochloric acid solutions, *International Journal of Electrochemical Science* **3** (2008) 806-818. https://doi.org/10.1016/S1452-3981(23)15485-X

[23] S. M. Abd El Haleem, S. Abd El Wanees, E. E. Abd El Aal, A. Farouk, Factors affecting the corrosion behavior of aluminum in acid solutions I. Nitrogen and/or sulfur-containing organic compounds as corrosion inhibitors for Al in HCl solutions, *Corrosion Science* **68** (2013) 1-13. http://dx.doi.org/10.1016/j.corsci.2012.03.021

[24] M. Abdallah, K. A. Soliman, M. Alfakeer, H. Hawsawi, A. M. Al-bonayan, S. S. Al-Juaid, M. S. Motawea, Expired antifungal drugs as effective corrosion inhibitors for carbon steel in 1 M HCl solution: Practical and theoretical approaches, *ACS Omega* **8** (2023) 34516-34533. https://doi.org/10.1021/acsomega.3c03257

[25] M. G. A. Saleh, M. Alfakeer, R. N Felaly, S. S. Al-Juaid, K. A. Soliman, S. Abd El Wanees, Modified chitosan as an effective inhibitor against the corrosion of C-steel in HCl solutions, *Journal of Adhesion Science and Technology* **39** (2025) 837-868. https://doi.org/10.1080/01694243.2024.2428401

[26] S. Hadisaputra, A. A. Purwoko, A. Hakim, N. Prasetyo, S. Hamdiani, Corrosion inhibition properties of phenyl phthalimide derivatives against carbon steel in the acidic medium: DFT, MP2, and Monte Carlo simulation studies, *ACS Omega* **7** (2022) 33054-33066. https://doi.org/10.1021/acsomega.2c03091

[27] M. J. Frisch, Gaussian 09 Rev. D.01. 2009: Wallingford, CT. H. Lgaz, H.-S. Lee, Computational exploration of phenolic compounds in corrosion inhibition: A case study of hydroxytyrosol and tyrosol, *Materials* **16** (2023) 6159. https://doi.org/10.3390/ma16186159

[28] M. G. A. Saleh, S.Abd El Wanees, 2,2'-Dithiobis(2,3-dihydro-1,3-benzothiazole) as an effective inhibitor for carbon steel protection in acid solutions, *Desalination and Water Treatment* **256** (2022) 242-252. https://doi.org/10.5004/dwt.2022.28374

[29] M. Alfakeer, S. Abd El Wanees, H. Hawsawi, S. S. Al-Juaid, A. M. Al-bonayan, M. Abdallah, S. S. Elyan, Controlling the oxide film destruction, metal dissolution, and H_2 generation on Al in acid solutions, *Desalination and Water Treatment* **290** (2023) 56-70. https://doi.org/10.5004/dwt.2023.29359

[30] S. M. Abd El Haleem, S. Abd El Wanees, A. Bahgat, Environmental factors affecting the corrosion behavior of reinforcing steel. V. Role of chloride and sulfate ions in the corrosion of reinforcing steel in saturated Ca $(OH)_2$ solutions, *Corrosion Science* **75** (2013) 1-15. https://doi.org/10.1016/j.corsci.2013.04.049

[31] S. Abd El Wanees, A. S. Al-Gorair, H. Hawsawi, S. S. Elyan, M. Abdallah, Investigation of anodic behavior of nickel in H_2SO_4 solutions using galvanostatic polarization technique. II. Initiation and inhibition of pitting corrosion by some inorganic passivators, *International Journal of Electrochemical Science* **16** (2021) 210548. https://doi.org/10.20964/2021.05.25

[32] A. S. Fouda, S. Rashwan, S. Emam, F. E. El-Morsy, Corrosion inhibition of zinc in acid medium using some novel organic compounds, *International Journal of Electrochemical Science* **13** (2018) 3719-3744. https://doi.org/10.20964/2018.04.23

[33] S. Abd El Wanees, S. Nooh, A. Farouk, S. M. Abd El Haleem, Corrosion inhibition of aluminum in sodium hydroxide solutions using some inorganic anions, *Journal of Dispersion Science and Technology* **43** (2021) 2021-2036. https://doi.org/10.1080/01932691.2021.1914647

[34] A.A. Atia, M.M. Saleh, Inhibition of acid corrosion of steel using cetylpyridinium chloride, *Journal of Applied Electrochemistry* **33** (2003) 171-177. https://doi.org/10.1023/A:1024083117949

[35] K.M. Shwetha, B.M. Praveen, B.K. Devendra, A review on corrosion inhibitors: Types, mechanisms, electrochemical analysis, corrosion rate and efficiency of corrosion inhibitors on

mild steel in an acidic environment, *Results in Surfaces and Interfaces* **16** (2024) 100258. https://doi.org/10.1016/j.rsurfi.2024.100258

[36] M. A. J. Mazumder, Synthesis, characterization, and electrochemical analysis of cysteine modified polymers for corrosion inhibition of mild steel in aqueous 1 M HCl, *RSC Advances* **9** (2019) 4277-4294. https://doi.org/10.1039/C8RA09833F

[37] N. H. Alharthi, El-Hashemy M. A., W. M. Derafa, I. O. Althobaiti, H. A. Altaleb. Corrosion inhibition of mild steel by highly stable polydentate Schiff base derived from 1,3-propane diamine in aqueous acidic solution, *Journal of Saudi Chemical Society* **51** (2022) 1935-1949. https://doi.org/10.1016/j.jscs.2022.101501

[38] A. S. Al-Gorair, M. S. Al-Sharif, S. S. Al-Juaid, M. G. A. Saleh, M. Abdelfattah, M. Abdallah, Bis(2-hydroxyethyl) ammonium dodecanoate and its constituents as inhibitors for Al corrosion and H_2 production in acid medium, *International Journal of Electrochemical Science* **19** (2024) 100452. https://doi.org/10.1016/j.ijoes.2023.100452

[39] A. S. Al-Gorair, R. N. Felaly, M. S. Al-Sharif, S. S. Al-Juaidd, M. G. A. Saleh, M. Abdallah, Inhibition of general and pitting corrosion of Ni in dilute sulfuric acid solutions utilizing some tetrazole derivatives, *International Journal of Electrochemical Science* **19** (2024) 100456. https://doi.org/10.1016/j.ijoes.2023.100456

[40] S. Abd El Wanees, M. Abdallah, A. S. Al-Gorair, F. A. A. Tirkistani, S. Nooh, R. Assi, Investigation of anodic behavior of nickel in H_2SO_4 solutions using galvanostatic polarization technique. I. Kinetics and thermodynamic approach, *International Journal of Electrochemical Science* **16** (2021) 150969. https://doi.org/10.20964/2021.01.15

[41] S. S. Abd El Rehim, S. M. Sayyah, M. M. El-Deeb, S. M. Kamal, R. E. Azooz, Adsorption and corrosion inhibitive properties of p(2-aminobenzothiazole) on mild steel in hydrochloric acid media, *International Journal of Industrial Chemistry* **7** (2016) 39-52. https://doi.org/10.1007/s40090-015-0065-5

[42] S. Abd El Wanees, A. S. Al-Gorair, H. Hawsawi, M. T. Alotaibi, M. G. A. Saleh, M. Abdallah, S. S. Elyan, Inhibition of pitting corrosion of C-steel in oilfield-produced water using some purine derivatives, *Desalination and Water Treatment* **269** (2022) 21-32. https://doi.org/10.5004/dwt.2022.28790

[43] S. Abd El Wanees, A. A. Keshk, Investigation of anodic behavior of nickel in H_2SO_4 solutions using galvanostatic polarization technique. IV. Initiation and inhibition of pitting corrosion by Cl^- ions and ethoxylated surfactants, *International Journal of Electrochemical Science* **16** (2021) 21087. https://doi.org/10.20964/2021.08.38

[44] S. Abd El Wanees, M. M. Kamel, M. Ibrahim, S. M. Rashwan, Y. Atef, M. G. Abd Elsadek, Corrosion inhibition and synergistic effect of ionic liquids and iodide ions on the corrosion of C-steel in formation water associated with crude oil, *Journal of Umm Al-Qura University Applied Science* **10** (2023) 107-119. https://doi.org/10.1007/s43994-023-00084-z

[45] M. G. A. Saleh, M. Alfaker, Y. Atef, S. S. Al-Juaid, A. Ghanem, M. M. Kamel, S. M. Rashwan, M. G. Abd Elsadek, S. Abd El Wanees, The utilization of ionic liquids as sustainable and eco-friendly inhibitors for corrosion protection of carbon steel in petroleum fields, *Inorganic Chemistry Communication* **167** (2024) 112699. https://doi.org/10.1016/j.inoche.2024.112699

[46] A. S. Al-Gorair, M. G. A. Saleh, M. T. Alotaibi, S. S. Al-Juaid, M. Abdallah, S. Abd El Wanees, Potentiometric and polarization studies on the oxide film repair and retardation of pitting corrosion on indium in an alkaline aqueous solution utilizing some triazole compounds, *Inorganic Chemistry Communication* **158** (2023) 111497. https://doi.org/10.1016/j.inoche.2023.111497

[47] E. E. Ebenso, D. A. Isabirye, N. O. Eddy, Adsorption and quantum chemical studies on the inhibition potentials of some thiosemicarbazides for the corrosion of mild steel in acidic

medium, *International Journal of Molecular Sciences* **11** (2010) 2473-2498. https://doi.org/:10.3390/ijms11062473

[48] M. K. Prashanth, C. B. Pradeep Kumar, B. S. Prathibha, M. S. Raghu, K. Y. Kumar, M. B. Jagadeesha, K.N. Mohana, H. Krishna, Effect of OH, NH_2 and OCH_3 groups on the corrosion inhibition efficacy of three new 2,4,5-trisubstituted imidazole derivatives on mild steel in acidic solutions: Experimental, surface and DFT explorations, *Journal of Molecular Liquids* **329** (2021) 115587. https://doi.org/10.1016/j.molliq.2021.115587

[49] M. Finšgar, A. Lesar, A. Kokalj, I. Milošev, A comparative electrochemical and quantum chemical calculation study of BTAH and BTAOH as copper corrosion inhibitors in near neutral chloride solution, *Electrochimica Acta* **53** (2008) 8287-8297. https://doi.org/10.1016/j.electacta.2008.06.061

[50] J. J. Martinez-Gonzalez, I. Tello-Salgado, M. Avilés-Flores, L. L. Landeros-Martínez, J. P. Flores-De los Ríos, J. G. Gonzalez-Rodriguez, Green corrosion and DFT studies of Ustilago maydis extract for carbon steel in sulfuric acid, *Journal of Molecular Structure* **1294** (2023) 136509. https://doi.org/10.1016/j.molstruc.2023.136509

[51] R. Omer, P. Koparır, L. Ahmed, M. Koparır, Computational determination the reactivity of salbutamol and propranolol drugs, *Turkish Computational and Theoretical Chemistry* **4** (2020) 67-75. https://doi.org/10.33435/tcandtc.768758

[52] A. Kokalj, N. Kovačević, On the consistent use of electrophilicity index and HSAB-based electron transfer and its associated change of energy parameters, *Chemical Physical Letters* **507** (2011) 181-184. https://doi.org/10.1016/j.cplett.2011.03.045